Research Article

Yawar Hussain*, Welitom Borges, Rogerio Uagoda, Cristiane Moura, Susanne Maciel, Omar Hamza, and Hans-Balder Havenith

Estimation of total groundwater reserves and delineation of weathered/fault zones for aquifer potential: A case study from the Federal District of Brazil

https://doi.org/10.1515/geo-2020-0226
received September 04, 2020; accepted January 16, 2021

Abstract: In the Federal District of Brazil, groundwater extraction is challenged by fractured aquifers with difficulty in identification of hydraulic traps and significant uncertainty in the estimation of recharge potential. This study aims to optimize the demarcation of new locations of tubular wells by the aid of geophysical investigation. In the first stage of this study, the total exploitable amount of groundwater were calculated from the information of the physical environment and the existing wells. Second, electrical resistivity tomography (ERT) method was carried out on the selected sites – based on their surficial characteristics. The possible hydraulic traps (where groundwater might exist) were identified from the inversion of the resistivity measured by the dipole–dipole array and from the delineation of the resultant conducting zones (including the weathered rocks and fractures). Using this approach, we predicted the position and number of tubular wells required and ranked them according to their potential productivity. The study provides a promising framework for investigating groundwater in fractured aquifers.

Keywords: ERT, fracture, groundwater, environmental factor, tubular wells

* **Corresponding author: Yawar Hussain,** Geology Department, Liège University, Liège, 4000, Belgium, e-mail: yawar.pgn@gmail.com
Welitom Borges, Cristiane Moura: Institute of Geosciences, University of Brasilia, Brasilia, 70910-900, Brazil
Rogerio Uagoda: Department of Geography, University of Brasilia, Brasilia, 70910-900, Brazil
Susanne Maciel: Planaltina Campus, University of Brasilia, Brasilia, 73345-010, Brazil
Omar Hamza: College of Science and Engineering, University of Derby, Derby, DE22 3AW, Derbyshire, United Kingdom
Hans-Balder Havenith: Geology Department, Liège University, Liège, 4000, Belgium

1 Introduction

Worldwide water demand is on the increase because of the growing global population and the unplanned urban growth that exerts stress on the aquifers [1] and other water resources. This situation leads to the search for new locations of wells installed in productive aquifers. In the case of hard rock aquifers, groundwater can be found in weathered and fresh rock interface, where the presence of joints, fractures, and fault zones (which are created by different chemical or tectonic processes) are expected to enable groundwater storage and transport [2–7]. Such aquifers can exist at variable depth; if the aquifer is deep, groundwater is pumped out by installing deep tubular wells (100–200 m). However, it is essential to conduct adequate groundwater exploration before installing these wells.

Prospecting for groundwater seeks to locate suitable quality and quantity of groundwater for extraction from an aquifer. This process involves the assessment of the recharge potential of the site in relation to the natural settings of the aquifers e.g., discontinuities/fractures, lineament, and quartz veins, which are attributed to the presence of highly productive aquifer [8,9]. However, such natural settings represent complex hydrological characteristics of aquifers. Therefore, groundwater prospecting in such regions is a challenging task where the presence of fractures as well as the intrinsic properties and physical environment of the site can play essential roles.

In addition to the traditional approaches used for assessing the physical environment of the hydrogeological setting of aquifers, geophysical methods offer the opportunity to detect the variation in ground conditions and the delineation of the zones that may appear as possible traps for groundwater in complex environmental conditions [6]. In particular, direct current, electrical resistivity tomography (ERT), which has been recognized as an economic and noninvasive geophysical technique with reasonable accuracy in the detection of hydrogeological features (fractures/weathered zones), can provide better structural information of highly heterogeneous geological features [10]. In ERT, a known value of current is passed through the earth, and a developed potential difference is observed which can be used for the subsurface analysis after inversion. ERT has been applied in many previous studies for the search of new groundwater prospects as well as for the monitoring of existing groundwater reservoirs [1,6].

These days, prospecting for groundwater is required more than ever. In the case of the Federal District of Brazil, unplanned urban growths in the surrounding regions of Brasilia are on the rise. In order to fulfill the rising water demands, new groundwater prospects are being investigated with consideration of the geology and the physical environment of the region. The city is constructed on a complex and heterogeneous groundwater flow system which constitutes both porous and fractured hydrological regimes having variable hydrogeological characteristics such as hydraulic conductivity and permeability.

This article presents a case study from the Federal District of Brazil, where ERT, as well as the existing geological and hydrogeological information of the study area, were utilized to optimize the demarcation of new tubular well locations. The study provided a description of the aquifer system of the area and then proposed and applied an integrated approach in which the recharge potential of the study area as well as the presence of fractures and weathered zones (conductive zones detected by ERT) were used as a criterion for the estimation of groundwater potential. The investigation was conducted on seven different sites in the *Condominio Solar da Serra*, Federal District of Brazil.

2 Description of the study area and methods

The study was conducted in *Condominio Solar da Serra*, located in the middle course of the *Taboca and Taboquinha Ribeirão* sub-basins (Figure 1). The area already has eight deep tubular wells installed, of which six of them are in

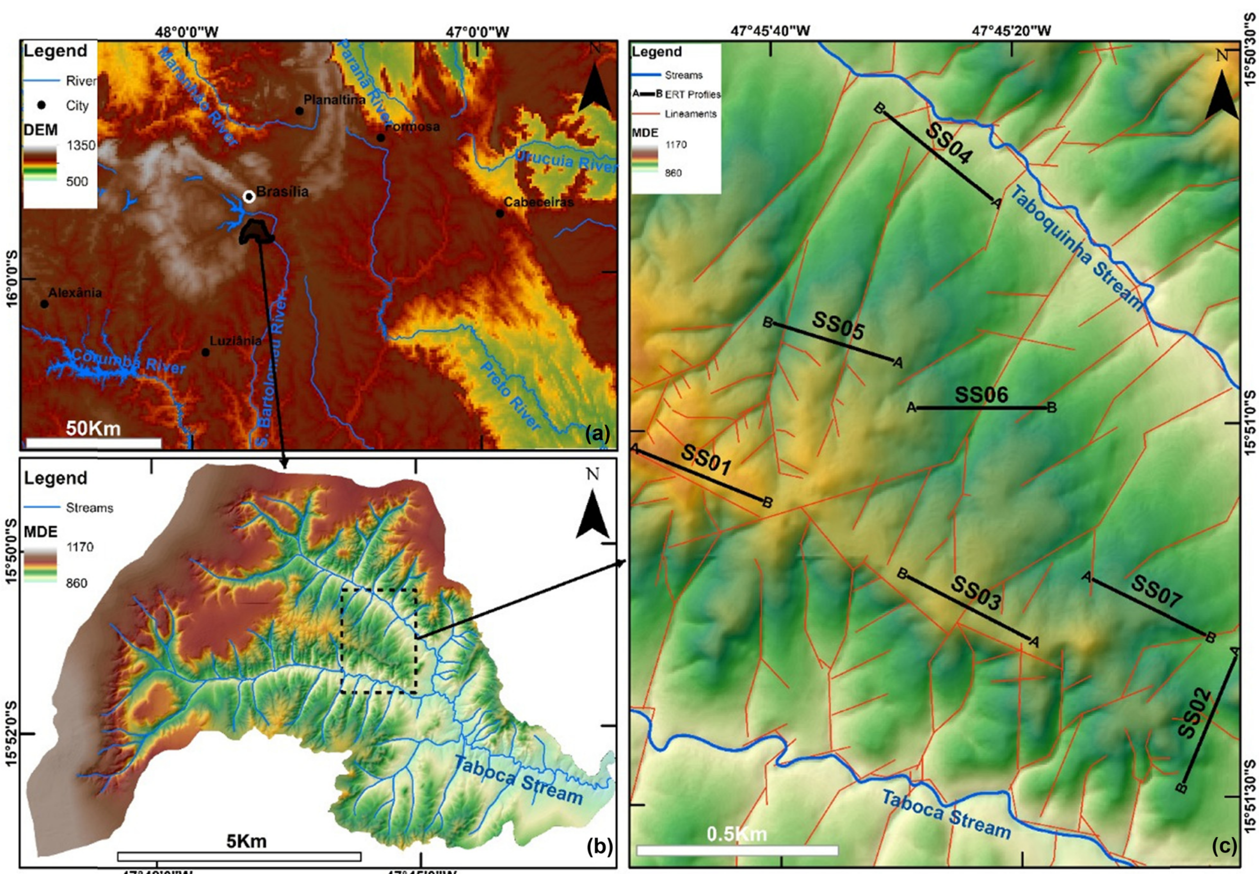

Figure 1: (a) Location of Brasilia on Brazil map, (b) location of *Condominio Solar da Serra* within the boundary Ribeirão Taboca-Taboquinha sub-basin, and (c) zoomed image of the study site along with the positions of ERT profiles and other hydrological features.

Table 1: Summary of the classification of domains, aquifer systems/sub-systems of the Federal District with respective mean flows [19]

Aquifer (system/subsystema)
Porous domain aquifer
Systems P1, P2, P3, and P4
Fracture domain aquifer
Paranoá system
Subsystem S/A
Subsystem A
Subsystem Q_3/R_3
Subsystem R_4
Subsystem PPC
Canastra system
Subsystem F
Subsystem F/Q/M
System BambuÍ
System Araxá

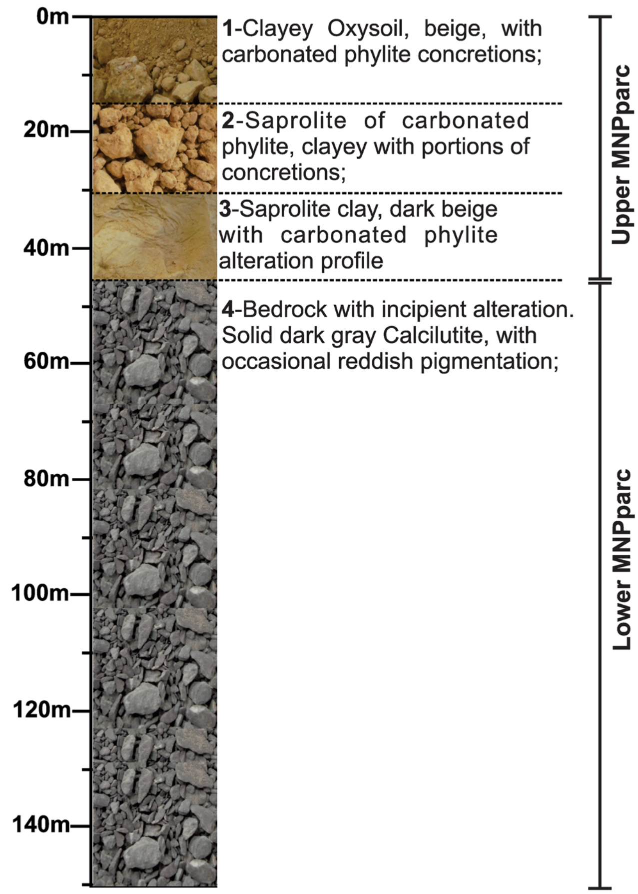

Figure 2: Lithosection of the area taken from the nearby tubular well. (1) Clayey oxisoil; (2) saprolite of carbonated phyllite; (3) fine yellow saprolite; and (4) bedrock [12].

operation. The region constitutes an aquifer system having moderate potential for production with an average flow rate of around 7.5 m^3/h (Table 1).

The Taboca and Taboquinha River sub-basins are located in the south and central portions of the Federal District and geologically constitute units of the *Paranoá* and *Canastra* groups. The Paranoá group is represented in the sub-basin by its *Ribeirão Contagem* (MNPparc) formation, which is further divided into two subunits as upper and lower (Figure 2). The lower subunit of Ribeirão formation consists of thin to medium-sized quartzites, white or light gray in color, well-sorted, mineralogically mature, usually very silicified, and having well-rounded grains. At the top, massive quartzites of the MNPparc superior formation found, characterized by the alternation of millimeter to centimeter levels of pure quartzites white to creamy color having millimeter to centimeter levels of ferruginous quartzites of medium particle size and gray in color. The MNPpacs *formation* is also divided into two subunits namely, upper and lower. The lower Sansão Stream formation subunit consists of homogeneous metarithmites with regular centimetric intercalations of metasilicates, metalamides, and fine quartzites that appear in different colors as gray, yellow, rose, or red. The Canastra group occupies about 70% of the area of the Taboca and Taboquinha Ribeirão sub-basins, which consists of phyllites, predominated by chlorite phyllites and quartz chlorite fengita filitos [11]. The lithosection and geological map of the area are presented in Figures 2 and 3, respectively.

Structurally, the area is located on the southeastern flank of the Brazilian structural dome. The NW–SE fracture-fault system controls the main drainage of the Taboca and Taboquinha streams that flow in the study area. The NE–SW system corresponds to the conjugate pair of the NW–SE system, which is in the predominant direction of the lineaments. The structural analysis of these systems, as well as the asymmetries of the drainage slopes shown on declivity map (Figure 3), were predominantly high angle fractures and faults with recessed blocks which are important features for the groundwater prospecting [13].

There are four large sets of residual soils in the Taboca and Taboquinha Ribeirões sub-basins [14]. These residual soils are deposited on the saprophytes of the Paranoá and Canastra groups. The soil of the area is divided as quartzarenic neosoils, latosols red-yellow, cambisols, and plintossolos (Figure 3). In the geomorphological context, the Taboca-Taboquinha sub-basin is located in the São Bartolomeu Rio Superior Course Unit. The Taboca-Taboquinha sub-basin is subdivided into seven geomorphological units as plateau plateau, elevated plateau, smooth section, dissection unit-high course, dissection unit-low course, dissection unit-lower middle course, dissection unit-middle higher course [15,16].

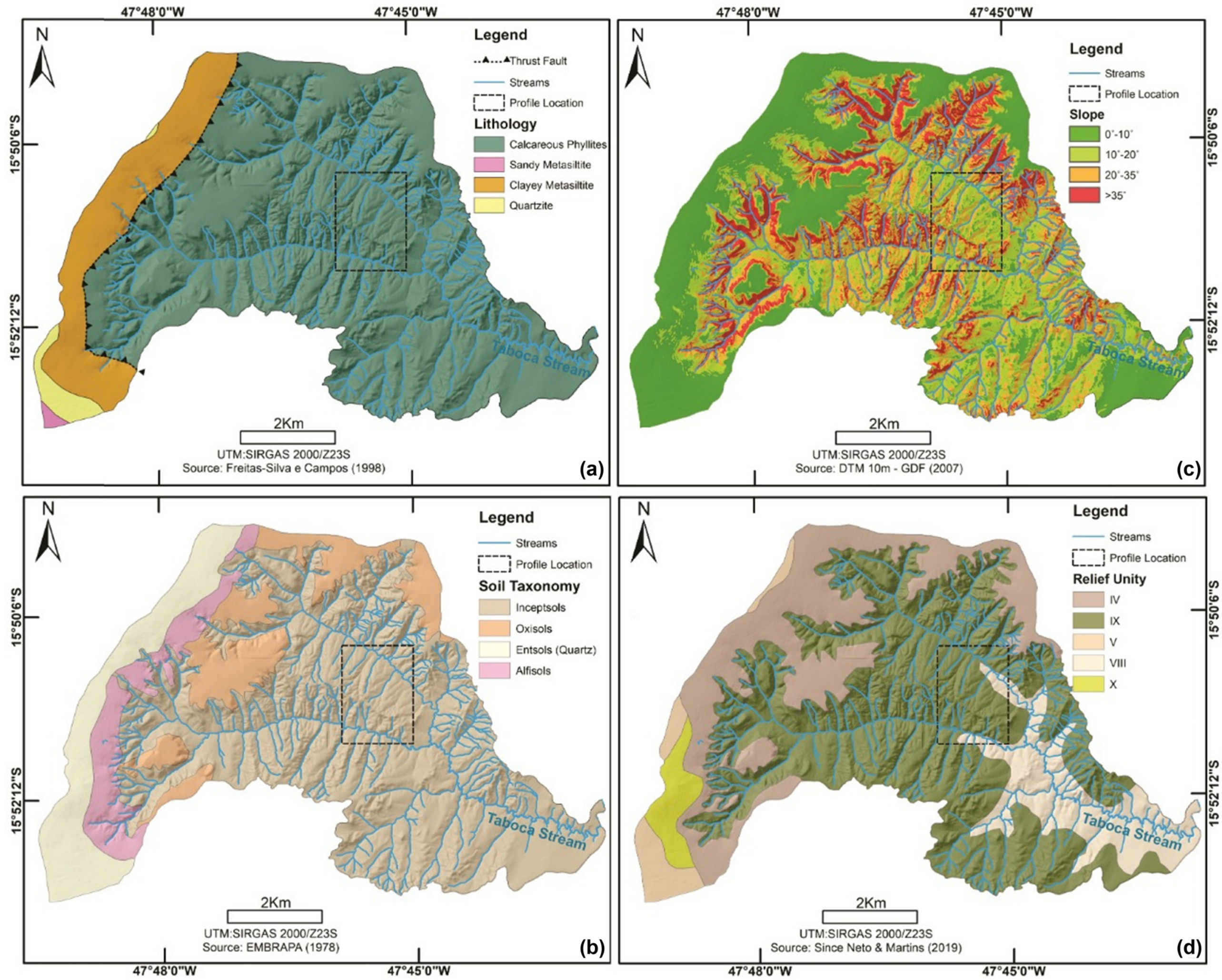

Figure 3: (a) Geology, (b) soil map, (c) declivity map, and (d) relief map of the Ribeirão Taboca-Taboquinha sub-basin.

The pioneering work on the hydrogeology of the Federal District was carried out by Romano and Rosas [17]. Subsequently, the contributions of Barros [18] were important for the assessment of groundwater in the region. After that, a succession of works has been developed in the region.

3 Aquifer domains

The Brazilian hydrogeological system is dominated by aquifers developed in fissures, covered by weathering layer of soils and altered rocks having variable hydrogeological characteristics (permeability and thickness). In Brasilia, two distinct aquifer domains are presented, namely: (i) Porous domain aquifers (PDA) and (ii) Fractured domain aquifers (FDA) (Table 1).

3.1 PDA

Since there are no sedimentary rocks with interstitial spaces, this domain consists of soils and the mantle of rock alteration (saprolite) in the area. Locally, the importance of aquifers in this domain is linked with several parameters, out of which only two are highlighted here: saturated thickness (b) and hydraulic conductivity (K), both are related with geology and geomorphology of their parent rocks. The domain is further subdivided into three systems: areas with latosols (Paranoá rocks), areas with structural soils (pelitic and carbonate rocks of the Paranoá group), and areas with cambisoils and neosoils (pelitic/claystone rocks of the Paranoá and Canastra groups). These sub-domains are named as P1, P2, P3, and P4, based on the “b” and “K” values (Table 1). The aquifers in the porous domain within the study area are of P3 and P4 subsystems with the argisoils/nitosoils and cambisoil/lithosoils, respectively. The P3 has a large thickness (>5 m) and low hydraulic conductivity, while P4 has smaller thicknesses (usually less than 1 m, but it can reach 2.5 m) and low hydraulic conductivity. The P4 water flow is very restricted, generally smaller than 300 L/h and shallow wells are installed in this aquifer, not present in the studied area but are quite common in the surroundings.

3.2 FDA

The FDA is associated with groundwater stored in the discontinuities related to faults, fractures, and joints in the absence of residual primary porosity in the rocks of the Paranoá group. The recrystallization of minerals and cementation completely obliterated the primary porosity originated by the metamorphic processes. The domain is represented by the systems of unconfined or confined aquifers, of restricted lateral extension, with strong heterogeneity and anisotropy responsible for the storage and circulation of deep groundwater. The hydrodynamic characteristics are variable in the domain depending on the type of rock. The density of the discontinuity in the rock body controls the hydraulic conductivity of the aquifers [20]. Generally, the fractured aquifers are pumped by means of deep tubular wells with depth varying from 100 to 200 m in the Federal District. The recharge occurs by the percolation of rainfall water. Other important factors that control the recharge depend on soil conditions, type of vegetation cover, soil thickness, and percentage of urbanized areas. Figure 4 presents a conceptual groundwater model in the area.

4 Method – ERT

The visible structural lineaments were extracted from the satellite images and digital terrain model, at a scale of 1:10,000. This information was used for the planning of electrical resistivity survey in the area (terrain conditions, environmental restrictions, etc.). Based on the preliminary analysis, seven areas were selected for conducting electrical resistivity profiles (Figure 5).

The electrical resistivity measurements were taken with a four-electrode system, two of which are used to pass electric current (I) to the ground and the other two are used to measure the potential difference (V) between them. By obtaining the potential difference and the current flowing in the medium, the apparent electrical resistivity of the medium is calculated which depends on the geometric factor (K), a function of the configuration of the electrodes [4]. Depending on the research objective, the electrodes' configuration can be conducted in several ways such as Wenner, pole–pole, pole–dipole, dipole–dipole, Wenner–Schlumberger, and gradient. Each arrangement has specific characteristics such as spatial resolution (dipole–dipole and pole–dipole), depth of investigation (pole–pole), and signal-to-noise ratio [22–26]. In the present study, the dipole–dipole (DD) electrode arrangement was adopted. Based on the study objectives, DD array is the most common array adopted for the groundwater prospecting in hard rocks due to good depth range but low signal-to-noise ratio [27]. The widespread voltage and current cables may result in good image resolution capabilities and may decrease in electromagnetic inductive noise [28–30]. Other advantages of using DD include

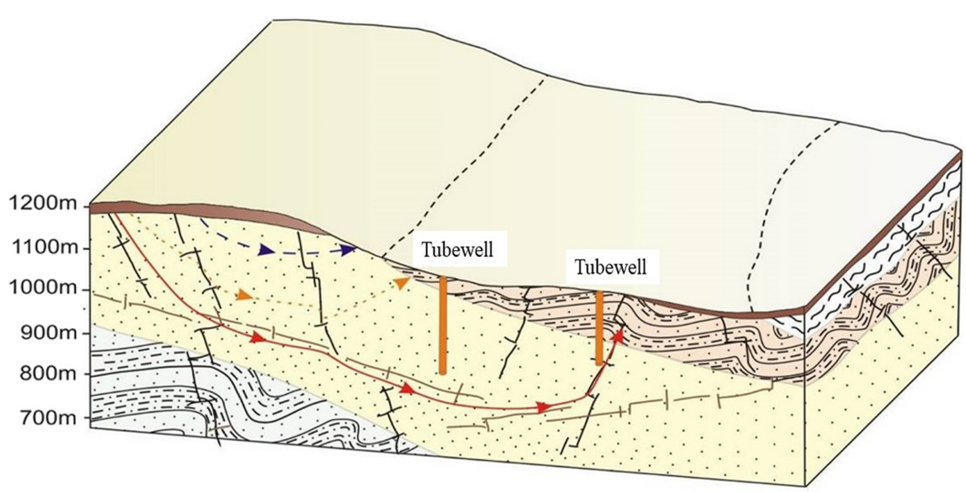

Figure 4: Schematic representation of the conceptual model of the aquifer system in the southern part of Brasilia [21].

Figure 5: Photographs illustrating the acquisition of ERT data on the selected sites in the study area.

delineation of lateral features and reciprocal measurements at shallow depth [31]. Data error and quality assessment can be made based on the reciprocal and forward measurements [32]. Okpoli [33] provided a detailed review of the advantages and disadvantages of the ERT arrays. Another approach was adopted in recent studies where multi-array configurations were used in the joint inversion [34,35].

The result of the acquisition is a set of electrical resistivity data obtained at various depths, forming a pseudo-section. This, in turn, reflects the behavior of the subsurface in response to the passage of electric currents. Each geological material shows a very broad range of resistivity, which depends mainly on the mineralogical composition of the rock, degree of weathering, the amount of fluids present in the pores of the rock, and the salinity of the fluid.

The acquisition of the geophysical data was executed along with eight profiles (Figure 5), each one of 350 m in length. One profile was not used because of poor signal-to-noise ration. In the field, the electrical resistivity data were collected with the electric roll-along technique, using the DD arrangement, with a spacing of 10 m between the electrodes. The data acquisition protocol with the multielectrode cables was elaborated in the software ELECTRE II, version 05.06.00, (IRIS Instruments) for acquisitions with 36 electrodes.

The measurements were taken in the dry season and salt water is poured to each electrode in order to increase the passage of current to the ground. The data were acquired with SYSCAL Pro 72 equipment (manufactured by IRIS Instruments), which consists of an interleaved acquisition module in multielectrode cables. Thirty-six stainless steel electrodes were used to inject current and measure the electric potential generated by the current flow in the subsurface.

ERT data were processed in a similar approach adopted by refs. [36,37]. The filtering and topographical correction on the dataset were performed in the PROSYS II software (IRIS Instruments). In order to determine the effective depth, the pseudo-sections of the electrical resistivity were inverted using the computer program RES2DINV (Geotomo Software). In our case, the resistivity values near the ground are high; therefore, a narrow model cell was used in RES2DINV program, where the width of the model block is kept as half of the electrode spacing for optimum result. The 2D model divides the subsurface into a series of blocks to determine the resistivity; its product is the apparent resistivity pseudo-sections that fit with the field data, using an inversion process based on the variation of the least square method. The results obtained were presented in the form of 2D resistivity profiles.

5 Results and discussions

5.1 Estimation of groundwater reserves

The entire area of the *Condominio Solar da Serra* is mainly in the form of aquifer subsystem F of the Canastra aquifer system. The subsystem F is one of the lowest production aquifers in the Federal District with an average flow rate of around 6,500 L/h. The best flow rates are obtained in neotectonic fault/fracture zones, especially in the NW–SE, NE–SW, NS, and EW directions. In addition, the small soil thickness (porous subsystem P4) overlying the subsystem F and low permeability of the phyllites cause great difficulties in the implementation of infiltration induced systems (artificial recharge).

The physical environment and climatic (rainfall) information are used in the determination of the deeper aquifers' flow as well as the elements for their sustainable management and extraction. Taking this into account, the main parameters for the volume calculations and flow rate estimation and the outflows of groundwater extraction of the study area are calculated (Table 2).

The average climatic conditions of the Federal District, which are marked by the strong seasonality, with two contrasting seasons are considered for the study area. The period between May and September is evidenced by low precipitation rate, low cloudiness, high evaporation rate, and low relative air humidity. The period between October and April presents distinct patterns, and the months from December to March constitute 47% of the annual precipitation. The average annual precipitation of the Federal District is about 1,500 mm; however, for estimation of water reserves, an average rainfall of 1,450 mm was considered.

According to ref. [38], about 12% of the total precipitation infiltrates the vadose zone and effectively reaches the saturated zone. This is considered for the areas occupied by subsystem P1; however, for the subsystem P4, a value of 8–9% is determined based on the physical environment of the area.

The total area of the *Condominio Solar da Serra* is 250.99 ha (2,509,900 m^2), 63.2% of which is destined for residential, commercial lots, and institutional areas, and 36.8% is reserved for the green areas. Thus, for the calculation of the total exploitable reserve (TER) for the area, the green areas (923,500 m^2) plus 30% of the urbanized area (475,920 m^2) are used.

Table 2: Parameters used in the estimation of groundwater reserves of Condominio Solar da Serra

Average annual precipitation (AAP)	1,450 mm
Porous domain area P4 – 20 m thick	1,400,000 m^2
Area of fractured system-F	1,400,000 m^2
Effective recharge of the porous domain – P4 for the fractured system F (percentage)	8%
Percentage of the permanent reserve available (annual)	9%
Thickness of the shallow fractured domain	70 m
Index of fractures interconnected in the short interval of the fractured subsystem	1%
Pore spacing of lower zone	60 m
Index of interconnected fractures of the deep interval of the fractured subsystem deep interval	0.5%

In order to establish a sustainable exploitation rate, the following parameters for a conservative estimation are considered: (i) The whole area is covered by the porous system P4, represented by shallow changes; (ii) The entire area of the C*ondominio* is composed of the aquifer subsystem F; (iii) For the calculation of the renewable reserve of the subsystem F, the effective recharge rate of the porous system is 10% of the total annual precipitation.

Equation (1) is used to calculate the reserve renewed annually from the infiltration of rainwater through the unsaturated zone to the saturated zone of the porous system and from there to the saturated zone of the rocky fractured environment.

$$\mathrm{RrF} = A \times \mathrm{ERF} \times \mathrm{AAP}, \tag{1}$$

where RrF is the renewable reserve of subsystem F, A is the system area available for infiltration (green area + non-edificated area), ERF is the effective recharge percentage from the overlapping porous system, and AAP is the average annual precipitation. After substituting the values from Table 2 into the above equation (1), a numeric value of "RrF = 162,400 m^3/year" is obtained.

The water reservoir is permanently contained in the rock fracture systems of the Canastra aquifer subsystem. It is calculated for different depths as a function of the different interconnected fracture rates (IFr), which tend to decrease with depth due to the increase in the lithostatic pressure. Permanent reserve of system F (PrF) can be calculated using equation (2). Substituting the values from Table 2 into equation (2) gives PrF = 1,400,000 m^3.

$$\begin{aligned} PrF &= PrFs + PrFi \\ &= (A \times bs \times I_{fii}) + (A \times ps \times I_{dif}), \end{aligned} \tag{2}$$

where PrFs is the permanent reserve of system F, PrFi is the permanent reserve of system F inferior interval, A is the area of fractured domain, bs is the thickness of upper fracture zone, I_{fii} is the index of fractures having larger interconnection interval, ps is the pore spacing of lower zone, and I_{dif} is the index of deeper interconnected fractures.

For the location of the deep tubular wells in the investigated area, all the information regarding the physical environment as described above were obtained from the already installed seven wells in the considered area (Table 3). However, the assessment of the constructive and geological profiles of the wells are not available; the existing information mainly includes the well's depth and pumping rate as can be seen in Table 3.

5.2 Site selection by ERT

Based on the inverted resistivity, geological information of the ground was prepared along with each profile. Different resistivity zones such as low, medium, high, and very high resistivity are delineated on the inverted resistivity data. These resistivity zones are possibly associated with the soil, fine saprolite, coarse saprolite, and saturated saprolite (Figure 2). Along with these, on the inverted resistivity pseudo-sections, some features delineate having an opening on the ground and are labeled as the suspected fractured or weathered zones within the underlying bedrock. It is interesting to note that some of the profiles show the resistivity changes in the same geological layer as a function of depth which indicate the presence of heterogeneity. It is also found that on some of the profiles, that change from one layer to another is not abrupt and instead a progressive shift in resistivity values are shown indicating the absence of abrupt shift among the facies of weathered saprolite/rock. The detailed discussions on the delineated features of interests on the individual profiles are presented below.

The unprocessed apparent resistivity pseudo-section along with profile SS01 is shown in Figure 6a. It can be seen that there are very high resistivity values at the center, which are marked as an unknown anomaly. On profile SS01 (Figure 6b), two anomalous features of low resistivity were found which might be associated with the fractured structures in the subsurface with a possible presence of groundwater or clay. These clays might be associated with the fluvial deposition. This profile has three lithologies, namely dry soil, fine saprolite, and coarse saprolite, each having a different resistivity anomaly.

On profile SS02 (Figure 7a), two anomalous features of low resistivity were found which might be associated with the fractured structures in the subsurface as possible traps of groundwater accumulation. However, due to the inherent ambiguity of indirect investigation by geophysical methods, there are other possible explanations of the observed low resistivity zone. At the beginning of the profile, low resistivity vein is found. This zone may be associated with the presence of a fracture in saprolite – filled with the clay. This clay may be fluvial deposit by the water flow. This is also a potential recharge zone for the underlying deep aquifer depending on permeability of the material (proportion of coarse grained material). High resistivity saprolite (high permeability) is also found here.

Results of profile SS02 show a highly fractured subsurface flow system. Similar to SS01 profile, at the beginning of the profile filled fractured zone is observed, which present a potential area of aquifer recharge. Zones of different resistivity values can be seen; these variations in values may be created by differential degrees of weathering, the proportion of fine-grained, and the degree of saturation within the same saprolite layer. The migration of water may create the variations in saturation because of the pumping in the nearby tubular wells. This

Table 3: Data of existing wells in the area

Well	Name	UTM X	UTM Y	Time of operation (h)	Flow rate (m^3/h)	Depth (m)	Depth of pump (m)
1	Poço Solar 3	203908.87	8245181.94	18	2.9	150	70
2	Poço Praça B	205547.37	8245578.17	16	6.6	150	110
3	Poço Clube	205729.04	8244743.23	20	7.5	90	60
4	Poço Praça Colibri	205684.33	8245377.90	20	7.5	100	60
5	Poço do Trevo	204829.69	8245420.01	20	3.0	260	150
6	Poço da Portaria	203864.14	8245748.70	20	1.5	90	60
7	Poço Desativado	204549.00	8245907.00	20	2.4	150	90
Average					4.49		

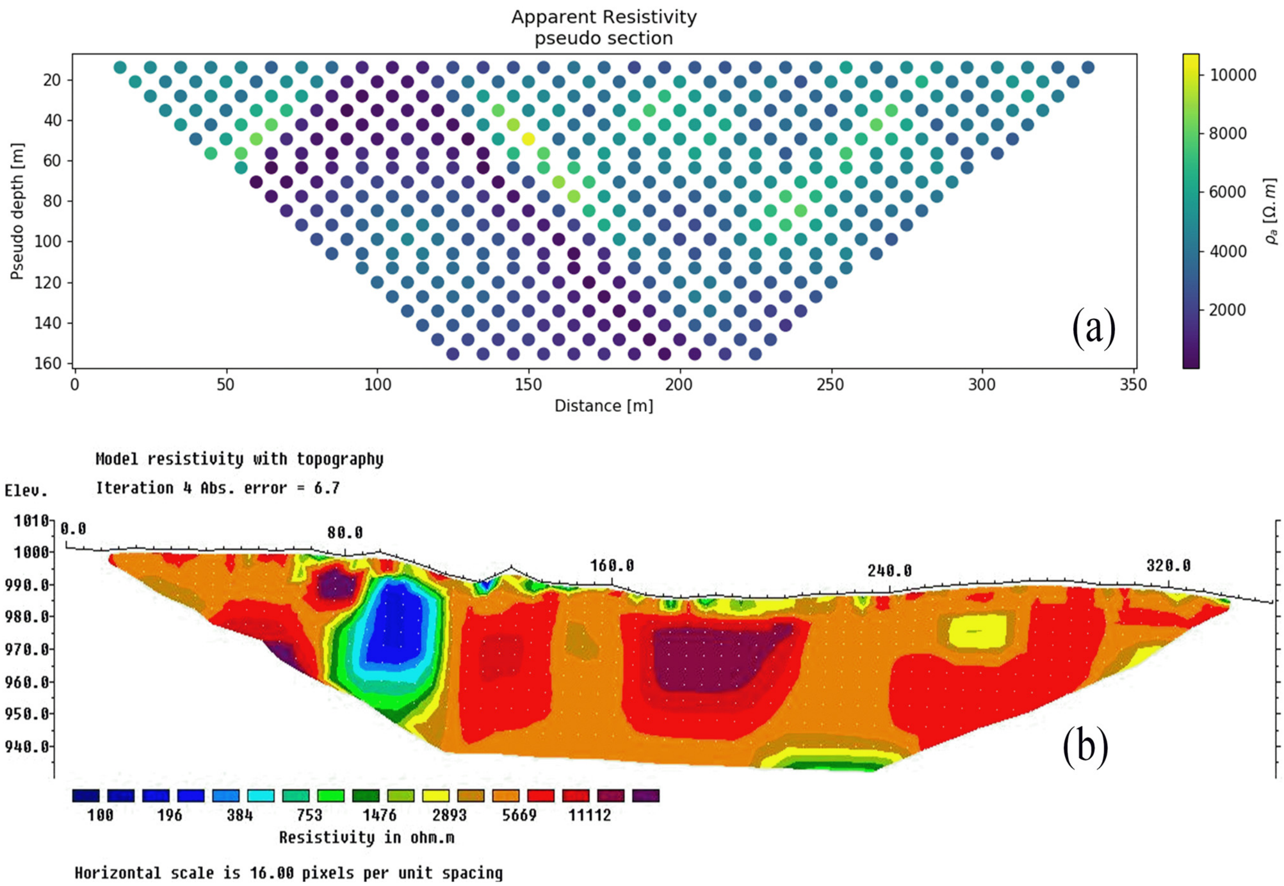

Figure 6: (a) Raw data record of profile SS01 and (b) the inverted resistivity cross-section.

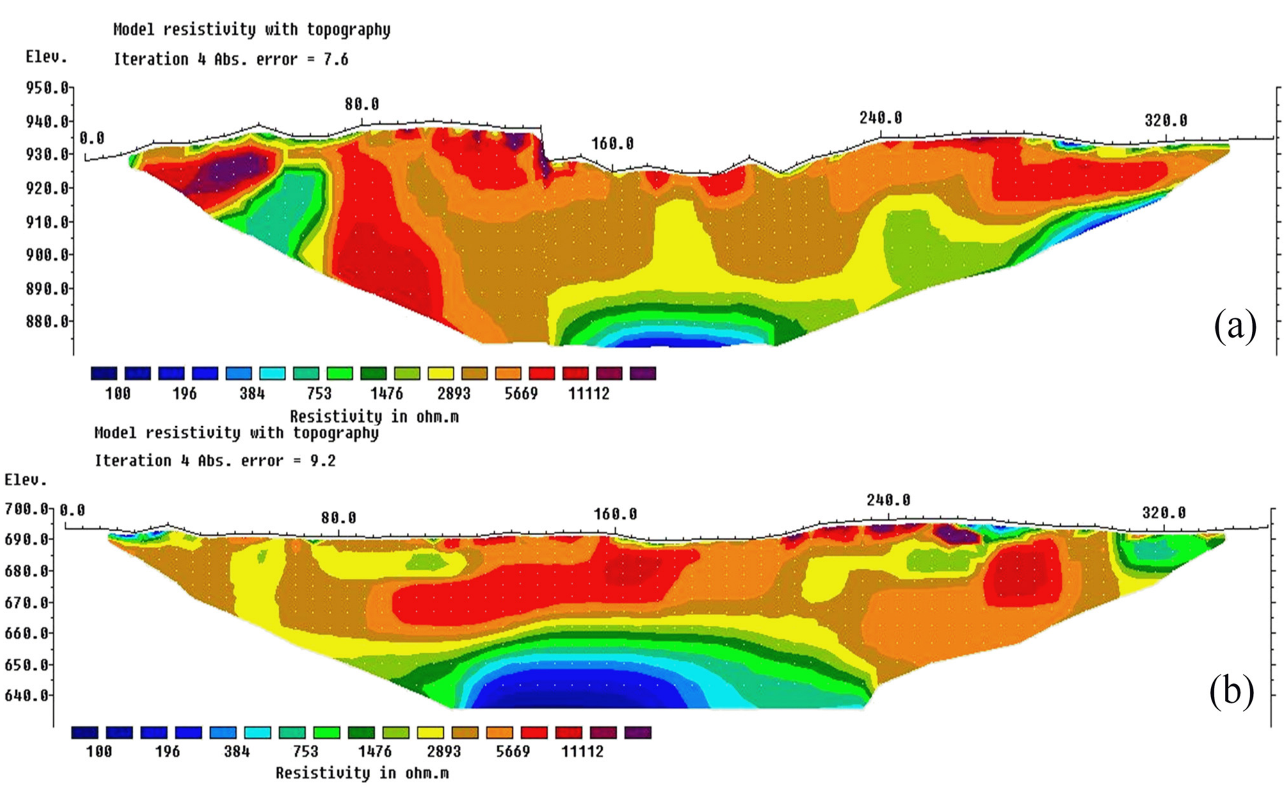

Figure 7: The inverted resistivity cross-sections of profiles: (a) SS02 and (b) SS03.

exploitation is further strengthened by the fact that ERT measurements were carried out in the dry season. On profile SS03 (Figure 7b), a medium to high resistivity anomaly was found which corresponds to a discontinuity coincident with relief lineage, which can store as well as recharge groundwater. Another possible explanation of the high resistivity anomaly near the end of the line may be related only to the presence of the coarse and dry material (saprolite). A contentious decrease in contour values within the same formation is observed on the middle to the right side of the profile SS03; this has also been reported in the literature by Soro et al. [39]. This may be related to seasonal aquifer which is pumped by the nearby well as explained above. In order to prove this hypothesis, measurement should be taken in the rainy seasons. Another possible reason for these resistivity variations may be linked with the variable degrees of weathering as explained above.

Profile SS03 (Figure 7b) shows very interesting results at the middle; there is a high resistivity propagating zone, below which there are layers with resistivity values showing that there is no abrupt change in the facies of same rock unit (saprolite). The high resistivity geoelectric anomaly corresponds to the presence of saprolite derived from phyllites, the layer below being interpreted as the presence of carbonaceous phyllites in the region. At a depth of 40 m there is a very low resistivity anomaly similar to the other profiles, which may be associated with the clayey saprolite – presenting a cap rock for the deeper deeper aquifer system. This profile shows a fractured opening at the ground at about 50 m from the start of the profile. The entire profile is horizontal, so it is not a favorable recharge site for the deeper aquifer.

Profile SS04 (Figure 8a) represents very similar favorable groundwater development conditions such as the presence of fractured opening at the surface, topographic depression, and the presence of clayey saprolite (cap rock) at shallow depth. These hydrogeological conditions are observed on profiles SS05, SS06, and SS07. Another possible explanation of the presence of such a low resistivity zone is the absorption of current by the layer above. In order to prove it drilling of borehole is recommended. It should be noted that the surface features of high resistivity, sometimes ellipsoidal, are associated with the presence of rainwater drainage network structures in the high resistivity geoelectric layer which may be associated with the presence of saprolite. Profile SS05 (Figure 8b) shows the presence of

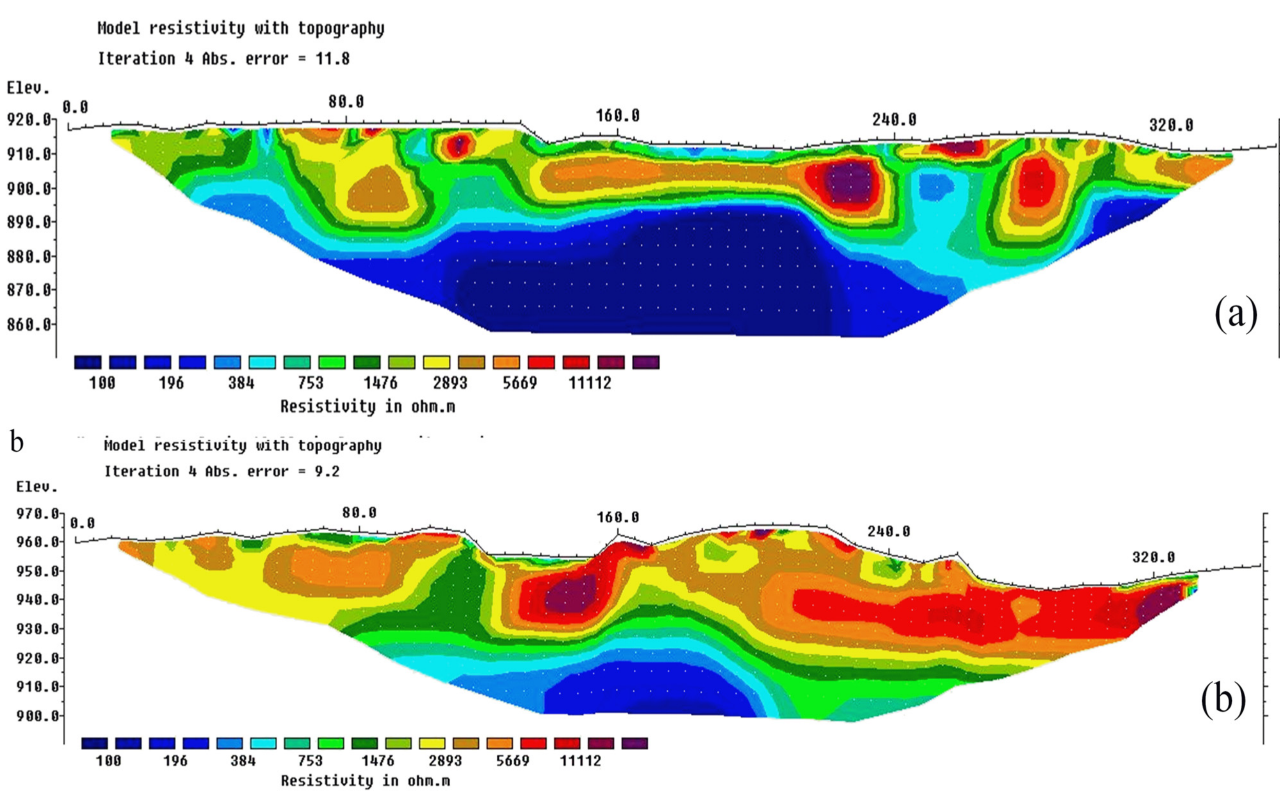

Figure 8: The inverted resistivity cross-sections: (a) SS04 and (b) SS05.

clayey saprolite associated with the domain of low resistivity. Therefore, this suggestion should be further confirmed by drilling (well) at the anomaly at 170 m away from the beginning of the profile SS06.

The discontinuities on profile SS07 suggest the presence of structures of interest, and this hypothesis can be investigated at a distance of 170 m from the beginning of profile SS06 (Figure 9b). This site presents a good topographic depression which can lead to holding of rainfall water which can infiltrate to the vadose zone and reach the saturated zone. Profile SS05 (Figure 8b) shows a very well defined and contentious soil layer. Below this soil layer is a coarse-grained dry saprolite layer (high permeability), which provides a pathway for the aquifer recharge. Below this layer comes a very low resistivity stratum which may be associated with the clayey saprolite – a potential cap rock at shallow depth for the deeper aquifer. At the beginning of the profile, similar to other sites, a fractured zone is delineated, which further enhances its suitability for the installation of the tubular well. From the beginning to the middle of the profile, there is very little topographic variation; however, from the middle to end, there is a considerable topographic variation.

From the results obtained by the adopted methodology, i.e., the application of 2D models of resistivity by inversion at seven locations, it was possible to identify the optimum distribution of the tubular wells. The wells' installation in the area is recommended based on the presence and ground opening of fractures, and presence of topographic depressions. These include the fractured or the conductive zones with possible recharge areas for the deeper aquifer, including any surficial features such as depression where rainfall water can accumulate. In total, seven tubular wells were suggested, and their proposed locations were prioritized as low, medium, and high depending on the analyzed data.

The profile SS01 has a high priority ranking based on the presence and surficial opening of the fracture; however, because of horizontal topography, an overall intermediate priority for the groundwater development is assigned to this site. The site of profile SS02 is ranked as high installation priority based on all the individual parameters (i.e., fracture, coarse saprolite, and depression).

Similar criteria were used to rank profiles SS03, SS04, SS05, SS06, and SS07, where the installation of two medium priority wells are recommended (based on the

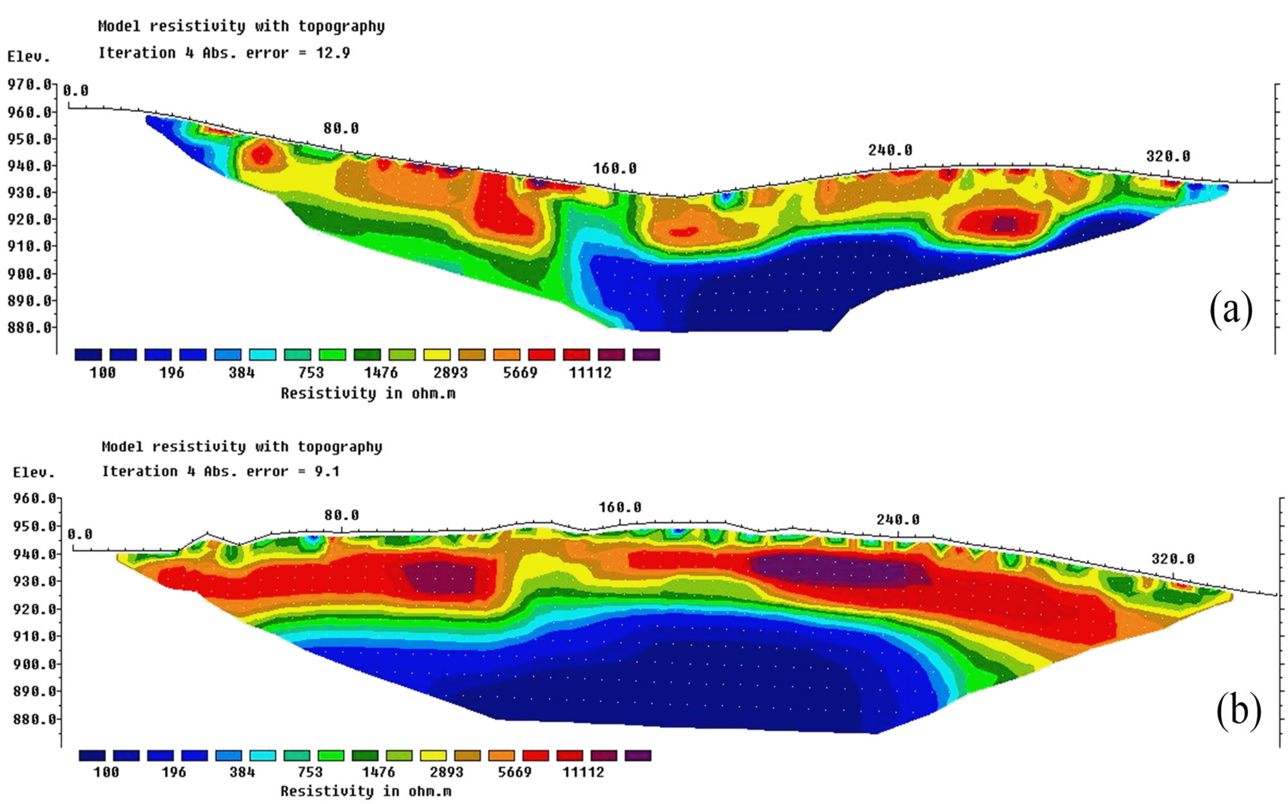

Figure 9: The inverted resistivity cross-sections: (a) SS06 and (b) SS07.

presence of the observed anomalous features). Accordingly, the location for the installation of a deep tubular well at 170 m from the beginning of the profile is suggested.

On the site of profile SS07, there are three lithologies interpreted as dry soil, dry saprolite, and clayey saprolite. In terms of the topographic and fractured zone, it is labeled as a high priority region. Profile SS07 also presents potential structures for surface water accumulation. Therefore, it is a recommended position for the installation of a tubular well in the region with lowest resistivity values, which is located at 150 m from the beginning of the ERT profile.

6 Conclusions and recommendations

In this paper, we presented a case study on the use of the geophysical approach (ERT) to identify new potential tubular wells and determined the recommended locations within the considered site (in the Federal District of Brazil).

The study demonstrated the ability to utilize the ERT inverted resistivity profiles accompanied with the geological information of the ground to conduct the following: (i) The development of site selection criteria (for potential tubular wells) based on the presence and surficial opening of the fracture; such prioritization criteria can increase the chances of success in the search for local groundwater. (ii) To exploit groundwater exclusively in the condominium tract and predict the maximum flow rate (e.g., in our case study, this was 39.5 m^3/h – considering 20 h of daily pumping). (iii) To estimate the optimum number of tubular wells required, based on the prediction of flow rate. For example, if the new wells reach the average flow rate of the aquifer subsystem F, 5–6 tubular wells (accurately constructed and operated) will be sufficient to reach the safe considered flow.

The approach presented in this study provides a promising framework for investigating and extracting groundwater in regions underlain by fractured aquifers. Overall, the study strengthens the idea that geophysical methods can aid groundwater exploration in challenging geological settings. Therefore, this approach is recommended to be carried out on any similar environments (hard rock), which would ensure that the use of ERT inverted resistivity profiles accompanied with the geological information optimizes both the position and production of tubular wells. For future work, coupled numerical modeling informed by geophysical, geological, hydrological, and meteorological data should be considered for more accurate estimation of wells' production.

Acknowledgments: The authors are most grateful to Dr. Eloi Campos of UnB and Regulatory Agency for Water, Energy, and Basic Sanitation of the Federal District of Brazil (ADASA) for providing the resistivity data and other related information.

Author contributions: Conceptualization, Y.H.; methodology, Y.H.; software, Y.H. and W.B.; writing-original draft preparation, Y.H.; writing-review and editing, Y.H., O.H., S.M., C.M., R.U., and H.-B.H. All authors have read and agreed to the published version of the manuscript.

Conflict of interest: Authors state no conflict of interest.

Data availability statement: Data is availbale on request to yawar.pgn@gmail.com.

Reference

[1] Hussain Y, Ullah S, Akhter G, Aslam AQ. Groundwater quality evaluation by electrical resistivity method for optimized tubewell site selection in an ago-stressed Thal Doab Aquifer in Pakistan. Model Earth Syst Environ. 2017;3(1):15.

[2] Xu S, Sirieix C, Riss J, Malaurent P. A clustering approach applied to time-lapse ERT interpretation – case study of Lascaux cave. J Appl Geophys. 2017;144:115–24.

[3] Watlet A, Kaufmann O, Triantafyllou A, Poulain A, Chambers JE, Meldrum PI, et al. Imaging groundwater infiltration dynamics in the karst vadose zone with long-term ERT monitoring. Hydrol Earth Syst Sci. 2018;22(2):1563–92.

[4] Guo W, Liu S, Liu Y, Chen S. Application of electrical resistivity imaging to detection of hidden geological structures in a single roadway. Open Geosci. 2020;12(1):1083–93.

[5] Rizzo E, Giampaolo V, Capozzoli L, Grimaldi S. Deep electrical resistivity tomography for the hydrogeological setting of Muro Lucano Mounts aquifer (Basilicata, Southern Italy). Geofluids. 2019:6594983.

[6] Hasan M, Shang Y, Jin W, Akhter G. Geophysical investigation of a weathered terrain for groundwater exploitation: a case study from Huidong County, China. Explor Geophys. Data 2020;52(3):273–93.

[7] Muzirafuti A, Boualoul M, Barreca G, Allaoui A, Bouikbane H, Lanza S, et al. Fusion of remote sensing and applied geophysics for sinkholes identification in Tabular Middle Atlas of Morocco (the Causse of El Hajeb): impact on the protection of water resource. Resources. 2020;9:51.

[8] Magowe M, Carr JR. Relationship between lineaments and ground water occurrence in western Botswana. Ground Water. 1999;37(2):282.

[9] Kuznetsov M, Viero AP, Sorek S, Roisenberg A, Ronen D. Modeling the flow pattern at the fractured granites in Porto Alegre, Brazil. Transp Porous Med. 2014;101(3):413–36.
[10] Redhaounia B, Ilondo BO, Gabtni H, Sami K, Bédir M. Electrical resistivity tomography (ERT) applied to Karst carbonate aquifers: case study from Amdoun, northwestern Tunisia. Pure Appl Geophys. 2016;173(4):1289–303.
[11] Campos JEG, Dardene MA, Freitas-Silva FH, Martins-Ferreira MAC. Geologia do Grupo Paranoá na Porção Externa da Faixa Brasília. Braz J Geol São Paulo. 2013;43(3):461–76.
[12] ADASA. Plano de Gerenciamento Integrado de recursos Hídricos do Distrito Federal – PGIRH. [Internet]; 2007. Available from: www.pgirh.df.gov.br
[13] Szűcs P, Szabó NP, Zubair M, Szalai S. Innovative hydrogeophysical approaches as aids to assess hungarian groundwater bodies. Appl Sci. 2021;11(5):2099.
[14] EMBRAPA. Brasilia: Empresa Brasileira de Pesquisa Agropecuária. Sistema brasileiro de classificação de solos; 2013. p. 353
[15] Novaes Pinto M. Caracterização geomorfológica do Distrito Federal. Novaes Pinto M (org). Cerrado: caracterização, ocupação e perspectivas. Brasília: Editora UnB; 1994. p. 285–320.
[16] Novaes Pinto M. Superfícies de aplainamento do Distrito Federal. Rev Bras Geogr. 1987;49(2):9–26.
[17] Romano O, Rosas JGC. Água subterrânea para fins de abastecimento de água e irrigação no Distrito Federal. Congresso Brasileiro Geologia, 24. Anais., Brasília: SBG; 1970. p. 313–33.
[18] Barros JGC. Caracterização geológica e hidrogeológica do Distrito Federal. Cerrado. 2a ed. UnB/SEMATEC; 1994. p. 265–83.
[19] Campos JEG, Freitas-Silva FH. Arcabouço hidrogeológico do Distrito Federal. In: Simp XII. Geol. Centro-Oeste. Boletim de Resumos. Brasília; 1999. p. 113.
[20] Campos JEG. Hidrogeologia do Distrito Federal: bases para a gestão dos recursos hídricos subterrâneos. Revista Brasileira de Geociências. 2004;34(1):41–8.
[21] Lousada EO, Campos JEG. Proposta de modelos hidrogeológicos conceituais aplicados aos aquíferos da região do Distrito Federal. Revista Brasileira de Geociências. 2005;35(3):407–14.
[22] Hussain Y, Hamza O, Cárdenas-Soto M, Borges WR, Dou J, Rebolledo JFR, et al. Characterization of Sobradinho landslide in fluvial valley using MASW and ERT methods. REM Int Eng J. 2020a;73(4):487–97.
[23] Park S, Yi M, Kim J, Shin SW. Electrical resistivity imaging (ERI) monitoring for groundwater contamination in an uncontrolled land fill, South Korea. J Appl Geophys. 2016;135:1–7.
[24] Martorana R, Capizzi P, D'Alessandro A, Luzio D. Comparison of different sets of array configurations for multichannel 2D ERT acquisition. J Appl Geophys. 2017;137:34–48.
[25] Samouëlian A, Cousin I, Tabbagh A, Bruand A, Richard G. Electrical resistivity survey in soil science: a review. Soil Tillage Res. 2005;83(2):173–93.
[26] Demirel S, Roubinet D, Irving J, Voytek E. Characterizing near-surface fractured-rock aquifers: insights provided by the numerical analysis of electrical resistivity experiments. Water. 2018;10(9):1117.
[27] Belle P, Lachassagne P, Mathieu F, Barbet C, Brisset N, Gourry JC. Characterization and location of the laminated layer within hard rock weathering profiles from electrical resistivity tomography: implications for water well siting. Geol Soc London Spec Publ. 2019;479(1):187–205.
[28] Dahlin T, Zhou B. A numerical comparison of 2-D resistivity imaging with 10 electrode arrays. Geophys Prospect. 2004;52:379–98.
[29] Fabregat I, Gutiérrez F, Roqué C, Comas X, Zarroca M, Carbonel D, et al. Reconstructing the internal structure and long-term evolution of hazardous sinkholes combining trenching, electrical resistivity imaging (ERI) and ground penetrating radar (GPR). Geomorphology. 2017;285:287–304.
[30] Pazzi V, Ceccatelli M, Ciani L, Patrizi G, Guidi G, Cappuccini L, et al. Analysis of the influence of the GPS errors occurred while collecting electrode coordinates on the electrical resistivity of Tumuli. Sensors. 2020;20(10):2966.
[31] Parasnis DS. Reciprocity theorems in geoelectric and geoelectromagnetic work. Geoexploration. 1988;25:177–98.
[32] Wilkinson PB, Loke MH, Meldrum PI, Chambers JE, Kuras O, Gunn DA, et al. Practical aspects of applied optimized survey design for electrical resistivity tomography. Geophys J Int. 2012;189:428–40.
[33] Okpoli CC. Sensitivity and resolution capacity of electrode configurations. Int J Geophys. 2013
[34] Bharti AK, Pal SK, Priyam P, Kumar S, Shalivahan PKY. Subsurface cavity detection over Patherdih colliery, Jharia Coalfield, India using electrical resistivity tomography. Environ Earth Sci. 2016;75(5):1–17.
[35] Bharti AK, Pal SK, Priyam P, Pathak VK, Kumar R. Detection of illegal mine voids using electrical resistivity tomography: the case-study of Raniganj coalfield (India). Eng Geol. 2016;213:120–32.
[36] Hussain Y, Uagoda R, Borges W, Nunes J, Hamza O, Condori C, et al. The potential use of geophysical methods to identify cavities, sinkholes and pathways for water infiltration. Water. 2020b;12:2289.
[37] Hussain Y, Uagoda R, Borges W, Prado R, Hamza O, Cárdenas-Soto M, et al. Detection of cover collapse doline and other epikarst features by multiple geophysical techniques: case study of Tarimba Cave, Brazil. Water. 2020c;12:2835.
[38] Carmelo AC. Caracterização de aquíferos fraturados por integração de informações geológicas e geofísicas. (PhD thesis). Brasília, DF, Brazil: Geociences Institut-University of Brasília; 2002. p. 179.
[39] Soro DD, Koïta M, Biaou CA, Outoumbe E, Vouillamoz JM, Yacouba H, et al. Geophysical demonstration of the absence of correlation between lineaments and hydrogeologically usefull fractures: case study of the Sanon hard rock aquifer (central northern Burkina Faso). J African Earth Sci. 2017;129:842–52.